Determination by X-Ray Photoelectron Spectroscopy of the Electronic State of Pd Clusters in Y Zeolite

Alexander Yu. Stakheev and Wolfgang M. H. Sachtler
V.N. Ipatieff Laboratory, Center for Catalysis and Surface Science, Northwestern University, Evanston, IL 60208, USA

X-Ray photoelectron spectroscopy (XPS) data of Pd clusters in NaY, MgY and HY zeolites show that the chemical shift of the Pd $3d_{5/2}$ line is dependent on the concentration of the protons and their position in the zeolite. The positive charge or 'electron deficiency' of the Pd particles is significant even for Pd/NaY which contains only the protons created by H_2 reduction of Pd^{2+} ions. In these samples the Pd $3d_{5/2}$ binding energy exceeds that of neutral Pd by *ca.* 0.4 eV. The positive charge of the Pd clusters is much higher in HY and MgY, reflecting the higher proton concentration in the supercages; the binding energy is shifted by 0.8 eV. Additional relevant information on the metal cluster environment is obtained from analysis of the Auger parameter of Pd. It decreases with increasing number of protons interacting with the Pd particles, and it increases upon substituting protons by polarizable ions, *e.g.* Na^+ or NH_4^+. These data are consistent with the model which suggests that metal–proton adducts, $[Pd_n-H_m]^{m+}$ with $m \geqslant 1$, are formed in proton-containing zeolites.

Numerous studies have been focused on the preparation, characterization and properties of metallic particles entrapped in zeolites. These systems are important industrial catalysts owing to their high catalytic activity in isomerization, hydrogenolysis, aromatization and hydrogenation–dehydrogenation.[1–5] The zeolite matrix not only imposes steric constraints for reacting molecules (shape-selective catalysis) and provides acid sites (bifunctional catalysis), but also affects the catalytic properties of encaged metal particles. The electronic state of the metal particles can be drastically modified by their interaction with electron-acceptor sites of the zeolite. Positively charged metal particles encaged in zeolites have been reported to exhibit higher catalytic activity towards hydrogenation[6–8] and hydrogenolysis,[9–12] different selectivity in the conversion of methylcyclopentane[12,13] and a stronger resistance to sulphur poisoning.[14]

Correlations between the positive charge on the metal particles and the concentration of Brønsted acid sites have been found recently.[15] It was shown that Brønsted acid sites act as electron acceptors, and decrease the electron density on the metal.[16] To rationalize the observed properties the model of electron-deficient metal–proton adducts, *e.g.* $[Pd_n-H_m]^{m+}$, has been proposed.[11,17] This model suggests that owing to the high metal–hydrogen bond strength it is conceivable that protons react with the metal particles forming Pd—H bonds. If the proton is attached to a metal particle, the positive charge in the resulting $[Pd_n-H]^+$ complex is no longer localized on the proton. The Pd atoms share this positive charge and become 'electron deficient' using Boudart's definition,[9] owing to delocalization of the electron density. The model does not imply total detachment of the proton from the oxygen ions. A Pd cluster interacting with a proton in a bridging position between the zeolite wall and the cluster is also considered as a metal–proton adduct.

Unfortunately, a quantitative or even semi-quantitative evaluation of the degree of electron deficiency of the metal particles remains difficult. Attempts to characterize the electronic state of the zeolite-encaged metals have been based on a number of physical and kinetic methods, including X-ray absorption spectroscopy, X-ray photoelectron spectroscopy (XPS), FTIR of adsorbed CO, and catalytic tests such as competitive hydrogenation of benzene and toluene.[18] However, the interpretation of these data is not unambiguous, because deviations of measured results from some reference can always be attributed to either of two causes: (1) different particle sizes and shapes, or (2) electron shift from the metal to the support. Changes in binding energies with respect to bulk metals have been reported[19–21] and attributed to a transfer of charge density from metal particles to the acid sites of the zeolites. However, more recently, a strong dependence of the binding energy on the metal particle size has been demonstrated.[22,23] For metal clusters on inert supports (SiO_2, carbon, Al_2O_3) three causes have been proposed to explain the observed shifts in photoelectron spectra and particle size:[24] (1) Coulomb interaction between the photoelectron and the positive charge left on the cluster; (2) a decrease of the screening energy (electronic response of the molecular environment of the atom to the creation of the core hole) in the final state; (3) changes in band structure due to the small cluster size leading to redistribution of electrons between orbitally distinct bands in the initial state.

The primary objective of the present research is to identify the electron transfer between the metal cluster and the zeolite Brønsted acid sites in Pd/Y in order to confirm the $[Pd_n-H_m]^{m+}$ adduct model. In previous research conducted in this laboratory FTIR of chemisorbed CO was used for this purpose.[25] In the present investigation the extent of metal cluster electron deficiency was determined as a function of zeolite proton concentration and position, using two sets of data: (*a*) the binding energy of Pd $3d_{5/2}$ and (*b*) the Pd Auger parameter (α').[26,27] To separate effects caused by varying particle sizes the following approaches have been used: (1) Neutralization of the acid sites with NH_3 or NaOH. Independent studies show that the metal particle size remains unaffected by this treatment.[13] (2) Comparison of samples with the same metal dispersion, but different concentrations and positions of acid sites; Pd/NaY, Pd/HY and Pd/MgY are used. (3) Identification of Pd particle size by independent methods, *e.g.* EXAFS and H_2 temperature-programmed desorption (TPD), as shown previously.[28,29]

Experimental

Sample Preparation

Three types of sample were used, *i.e.* Pd/HY, Pd/NaY and Pd/MgY. Pd/HY was prepared from Linde LZ-72 with an approximate unit cell formula of $H_{44.8}Na_{9.2}(AlO_2)_{56}(SiO_2)_{136}$.

Pd/NaY and Pd/MgY samples were prepared from Linde LZ-52 with an approximate unit cell formula $Na_{56}(AlO_2)_{56}(SiO_2)_{136}$.

MgY was prepared by ion exchange of dilute $Mg(NO_3)_2$ solution with an NaY slurry, followed by an ion migration procedure. Details of this preparation have been described elsewhere.[30] The loading of Mg^{2+} corresponded to ca. 16 ions per unit cell.

Palladium was introduced via ion exchange of a dilute solution (0.01 mol dm^{-3}) of $Pd(NH_3)_4(NO_3)_2$ with a zeolite slurry according to the procedure described elsewhere.[25] The Pd^{2+} loading corresponded to ca. 6.5 ions per unit cell (4 wt.%).

The ion-exchanged samples were calcined in flowing O_2 at a flow rate of 1200 cm^3 min^{-1} g^{-1} while the temperature was ramped at 0.5 °C min^{-1} from room temperature to 500 °C, and then held at the final temperature for 2 h.

Sample reduction, unless otherwise noted, was carried out in a 5% H_2–Ar mixture flow (170 cm^3 min^{-1} g^{-1}) while the temperature was increased at 8 °C min^{-1} to 350 °C and then held at the final temperature for 30 min.

Neutralization of Acid Sites in Reduced Samples

Reduced Pd/NaY samples free of acid sites were prepared by neutralization with NaOH and NH_3. For neutralization with NaOH after reduction the reactor was purged with wet Ar to saturate the zeolite with water, then placed in a glove box filled with N_2. The catalyst was reslurried in a deoxygenated NaOH solution (pH 11.5, 1000 cm^3 g^{-1} catalyst). After drying in N_2, the sample was loaded into the reactor, dehydrated in an Ar flow at 300 °C for 2 h, oxidized at 300 °C in flowing O_2 for 2 h and reduced in a 5% H_2–Ar mixture at 300 °C.

For neutralization with NH_3 after reduction the reactor was purged with an NH_3–Ar mixture (1/10) for 2 h. Physisorbed ammonia was eliminated by purging with Ar at 130 °C for 18 h. Subsequently, the sample was re-reduced in a 5% H_2–Ar mixture at 250 °C.

H_2 Chemisorption

Metal dispersion was measured by TPD. The experimental procedure has been described elsewhere.[11] H_{ads}/Pd ratios were obtained from integration of the TPD peak areas. Complete destruction of the Pd hydride phase was ensured by purging the sample for 20 min at room temperature (RT) in an Ar flow (200 cm^3 min^{-1} g^{-1}).

XPS Measurements

XP spectra were measured using a VG ESCALAB-5 spectrometer using unmonochromatized Al-$K\alpha_{1,2}$ radiation. The spectrometer was equipped with a high-pressure reaction cell to carry out sample pretreatment in various atmospheres at elevated temperatures. The sample was then transported to the analytical chamber of the spectrometer without contact with air. The adventitious carbon 1s line (285.0 eV†) was used as a reference for the energy scale. The binding energy of the Si 2p level was determined for pure zeolite and unreduced samples (103.5 eV); the charging effect in reduced samples was also cross-checked using the binding energy of that line. Values of the modified Auger parameter (α') for Pd were also determined using the kinetic energy of the X-ray excited M_5VV transition electrons and the binding energy of Pd

† 1 eV ≈ 1.602 × 10^{-19} J.

$3d_{5/2}$ level, as

$$\alpha' = E_b(3d_{5/2}) + E_k(M_5N_{45}N_{45})$$

The surface Pd/Si atomic ratio was estimated from the integral intensities of Pd 3d and Si 2p lines using the Wagner sensitivity factors.[31]

Samples for XPS studies were pressed in a hydraulic die to form thin, smooth pellets and placed in the high-pressure cell. Afterwards the sample was reduced in flowing H_2 at 150 °C for 30 min.

To investigate the Pd/NaY reduction process, the calcined sample was placed in the high-pressure cell and recalcined in flowing O_2 at 500 °C for 1 h. After initial spectra measurements, the sample was reduced stepwise at 50, 100, 120, 150, 200, 250, 300, 350 and 450 °C in a 5% H_2 in Ar flow. The sample was held at each temperature for 8–10 min. After each step it was transferred into the analytical chamber and spectra were recorded.

Results

Metal Distribution in the Samples

Tables 1 and 2 present the results from the XPS and TPD investigations. The XPS results show that the Pd/Si atomic ratios for all samples are close to the bulk value. This indicates that there is no surface enrichment of Pd and that the metal is homogeneously distributed.

Pd/NaY Reduction

Fig. 1 shows the Pd 3d spectrum of Pd/NaY reduced in H_2 at different temperatures, T_R. Reduction at $T_R \approx 100$ °C results in a shift of the Pd $3d_{5/2}$ line from 337.4–337.2 eV (corresponding to Pd^{2+} ions[20,32]) to 336.6 eV. Upon increasing T_R the Pd 3d line shifts further to lower binding energies. As shown in Fig. 2, two regions can be discerned: For $100 \leqslant T_R/°C \leqslant 200$ the binding energy does not change significantly. At higher T_R it abruptly decreases to 336.2 eV and then remains constant up to $T_R = 450$ °C.

In Fig. 3 the full width at half height (FWHH) of the Pd $3d_{5/2}$ line is plotted as a function of T_R. A sharp decrease of FWHH at $T_R \approx 150$ °C is noted.

The position of the Auger Pd M_5VV line changes in an analogous manner with T_R as shown in Fig. 4. There is no

Table 1 XPS and TPD data on Pd/NaY before and after neutralization

sample	Pd $3d_{5/2}$/eV	FWHH/eV	Pd/Si[a]	H_{ads}/Pd
before neutr.	336.2	2.1	0.042	0.62
neutr. with NaOH	335.9	2.1	0.041	0.63
neutr. with NH_3	335.8	2.2	0.047	0.60
bulk Pd	335.2	1.8	—	—

[a] Pd/Si bulk atomic ratio 0.048.

Table 2 XPS and TPD data on Pd/Y catalysts

sample	Pd $3d_{5/2}$/eV	FWHH/eV	Pd/Si[a]	H_{ads}/Pd
Pd/NaY	336.2	2.1	0.042	0.62
Pd/MgY	336.5	2.0	0.049	0.59
Pd/HY	336.5	2.1	0.041	0.63

[a] Pd/Si bulk atomic ratio 0.048.
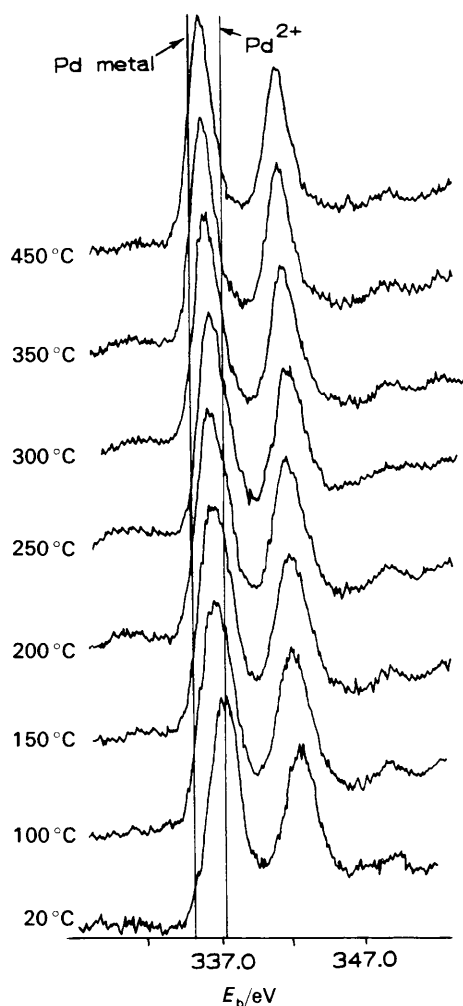
Fig. 1 Positions of the Pd 3d line at increasing reduction temperature for Pd/NaY

Fig. 3 Dependence of the Pd $3d_{5/2}$ FWHH on reduction temperature for Pd/NaY

$3d_{5/2}$ binding energy and the Pd M_5VV kinetic energy) is displayed in Fig. 5. Two distinct regions are discerned: (1) below 250 °C the average value of α' is equal to 661.6 eV; (2) above 300 °C it is equal to 662.3 eV and remains constant up to 450 °C.

significant change between 100 and 200 °C; however, in the region around 250 °C a marked shift to higher kinetic energies occurs. The shape of the Auger line also changes during reduction and becomes similar to that of the bulk metal after reduction at high temperature. The dependence on T_R of the modified Auger parameter (calculated on the basis of the Pd
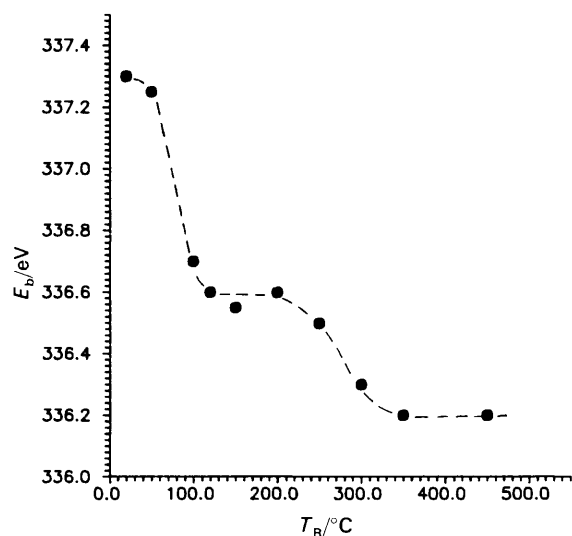

Fig. 2 Dependence of the Pd $3d_{5/2}$ binding energy on reduction temperature for Pd/NaY
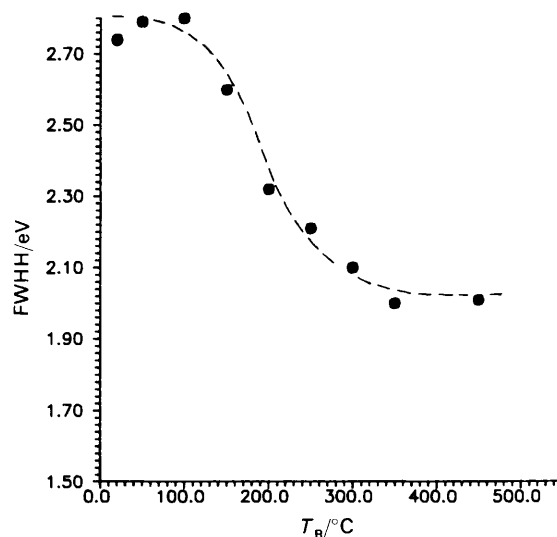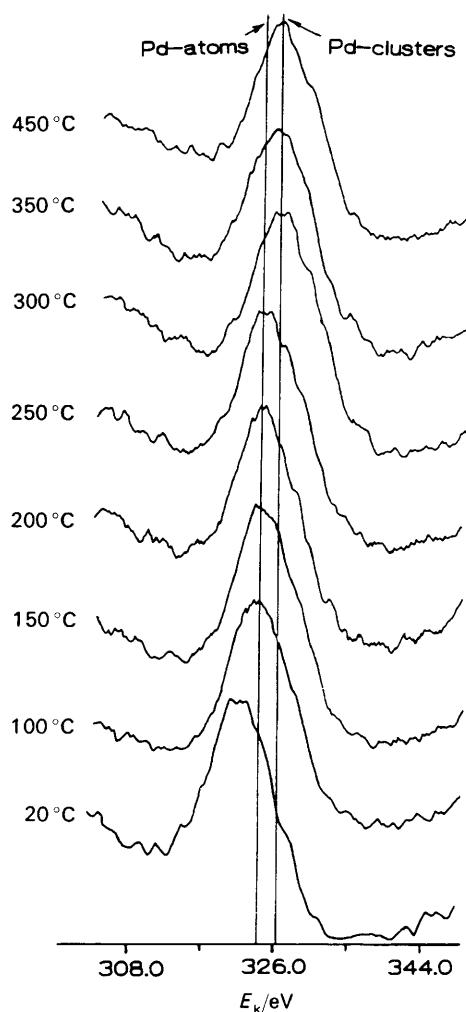

Fig. 4 X-Ray excited Pd M_5VV Auger line at different reduction temperatures for Pd/NaY
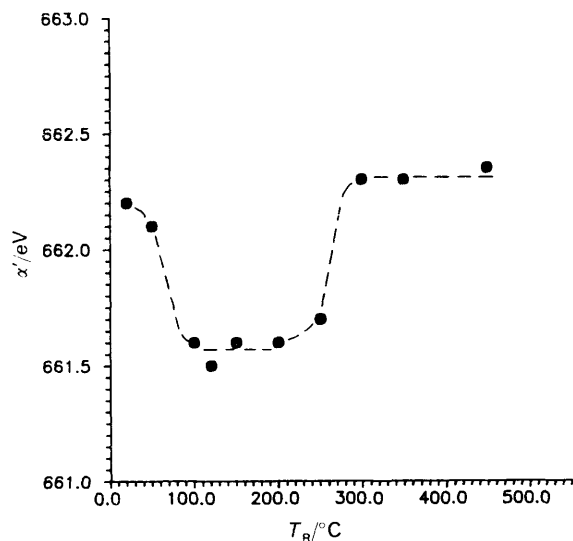
Fig. 5 Dependence of the Pd Auger parameter (α') on reduction temperature for Pd/NaY

Pd/NaY Neutralization

To evaluate the effect of neutralization on Pd/NaY, XPS measurements and TPD determinations of the metal dispersion have been carried out on the same sample before and after neutralization (Table 1). Neutralization does not significantly change the H_{ads}/Pd ratios or the Pd/Si XPS intensity ratios. Neutralization with either NH_3 or NaOH results in a shift of the Pd $3d_{5/2}$ line by 0.3–0.4 eV towards lower binding energy. Simultaneously, the Auger parameter changes significantly, it is sensitive to the neutralizing conditions: upon neutralization with NaOH α' increases by 0.3 eV, but after neutralization with NH_3 by 0.7 eV.

Comparison of Pd/NaY, Pd/MgY and Pd/HY

Results of XPS and TPD investigations are summarized in Table 2 and Fig. 6 and 7. The dispersions of Pd in all samples are approximately equal owing to the size constraint imposed by the zeolite matrix and similar temperature regimes during preparation. However, the Pd $3d_{5/2}$ binding energies in Fig. 6 differ considerably: binding energies of Pd $3d_{5/2}$ for Pd/HY and Pd/MgY are 0.4 eV higher than that for Pd/NaY.
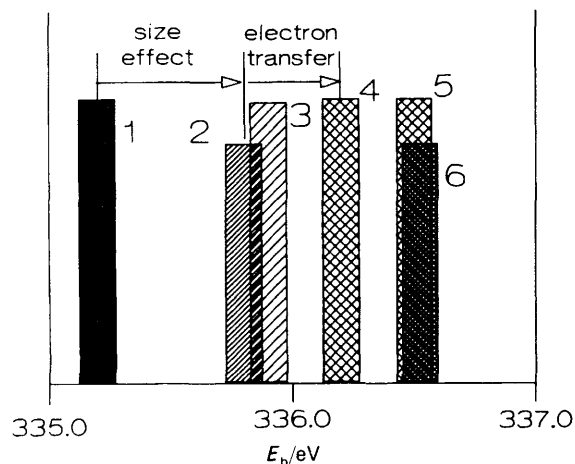
Values of the Auger parameters for Pd/HY and Pd/MgY in Fig. 7 also differ from that for Pd/NaY. In contrast to the binding energies these α' values are not equal for MgY and HY. The lowest value of 661.6 eV is observed for Pd/HY. For Pd/MgY the α' value of 662.0 eV is intermediate between those for Pd/HY and Pd/NaY.

Discussion

With XPS only the part of the zeolite closest to the surface is analysed. The depth of the zone probed by XPS can be estimated as follows. The electron mean free path (EMFP) for Pd 3d electrons determined experimentally and theoretically is ca. 2.6 nm in bulk SiO_2.[33] The void volume in faujasite is ca. 47%,[34] therefore the effective EMFP of Pd 3d electrons in zeolite Y can be roughly estimated as 5 nm. Taking into account that the unit cell constant in faujasite is 2.5 nm,[34] it follows that the major part of the XP signal is provided from two or three unit cells below the surface. The bulk and surface Pd/Si ratios of the present samples investigated show that the distribution of the metal in the zeolite microcrystals is homogeneous (Tables 1 and 2), i.e. the XPS information is not predominantly due to Pd particles at the external surface. This fact justifies considering the XPS information as being characteristic for the bulk of the zeolite microcrystals.

The data on Pd/NaY reduction will first be discussed in terms of the present knowledge of the elementary steps of metal particle formation in this zeolite. As the changes in the binding energy of Pd $3d_{5/2}$ and in the modified Auger parameter occur at the same T_R, it may be assumed that both shifts are caused by changes in the electronic structure of the Pd particles, rather than any spurious effects of differential charging.

The genesis of metal clusters in Pd/NaY has been studied by XRD,[35] TPO, TPR, TPD[28,29] and EXAFS.[36] It follows from these results that after calcination at 500 °C Pd^{2+} ions are located in the sodalite cages. During reduction with H_2 at $T_R \leqslant 250$ °C Pd atoms are formed, most of which remain in the small cages; at $T_R > 300$ °C they start migrating to supercages and form Pd_n particles.

Thus, XP signals in the first T_R region of 100–250 °C can be attributed to isolated atoms in small cages. Average values of the Pd $3d_{5/2}$ binding energy and of the Auger parameter for these species are 336.6 and 661.6 eV, respectively. Formation of Pd clusters at elevated temperatures causes an increase of α' and a decrease of the binding energy due to: (1) size effects (vide infra) and (2) changing interactions with the support.

Fig. 6 Positions of Pd $3d_{5/2}$ line for: 1, bulk Pd; 2, Pd/NaY neutralized with NH_3; 3, Pd/NaY neutralized with NaOH; 4, Pd/NaY reduced at 350 °C; 5, Pd/MgY reduced at 350 °C; 6, Pd/HY reduced at 350 °C; width of the bars corresponds to error bar
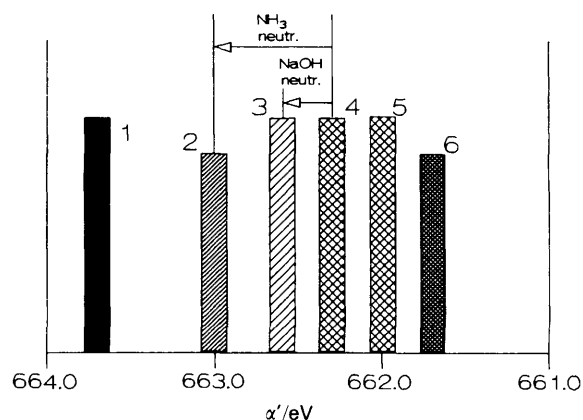

Fig. 7 Values of Pd Auger parameter for: 1, bulk Pd; 2, Pd/NaY neutralized with NH_3; 3, Pd/NaY neutralized with NaOH; 4, Pd/NaY reduced at 350 °C; 5, Pd/MgY reduced at 350 °C; 6, Pd/HY reduced at 350 °C; width of the bars corresponds to error bar

Average values of the Pd $3d_{5/2}$ binding energy and Auger parameter for Pd clusters are 336.2 and 662.3 eV, respectively. Considering the T_R dependence of the Pd $3d_{5/2}$ FWHH, it is remarkable that the abrupt decrease of this value occurs at a significantly lower temperature (ca. 150 °C) than the migration of Pd atoms to supercages (250–350 °C). We assume that this decline corresponds to the reduction of Pd^+ ions to Pd°. EPR and XPS data of Narayana et al. show that Pd/faujasite, when reduced at low T_R, contains measurable quantities of Pd^+ ions.[20] These authors also found that Pd^+ and Pd_m^{n+} clusters have similar Pd $3d_{5/2}$ binding energies, ca. 336.4 eV. This value is comparable to that determined in the present work for isolated Pd atoms (336.6 eV). This suggests that the presence of Pd^+ ions at reduction temperatures below 150 °C does not lead to the appearance of a new peak in the Pd 3d spectrum, but only increases the higher FWHH of the Pd $3d_{5/2}$ peak. The decrease of the FWHH value corresponds to the disappearance of these ions at elevated reduction temperatures.

The shift of the Pd $3d_{5/2}$ line for Pd clusters ($T_R > 300$ °C) with respect to the bulk metal value is ca. 1.0 eV. It is difficult to estimate contributions to this shift due to size effects and electron transfer from the metal to the support. An attempt to estimate the positive charge on the Pd clusters, using the approximation proposed by Wagner[26] and Thomas[37] (based on the shifts of the photoelectron and Auger lines vs. those of bulk metal) did not provide reliable results. This may be due to the complications arising from the involvement of two valence electrons in the Auger process for the Pd M_5VV as described by Wertheim.[38]

Nevertheless, we can estimate the positive charge on the Pd clusters caused by the formation of $[Pd_n-H_m]^{m+}$ by comparing the shifts of the Pd $3d_{5/2}$ line before and after neutralization of the Brønsted acid sites. Comparison of the H_{ads}/Pd ratios and the XPS Pd/Si atomic ratios before and after neutralization shows the absence of any substantial change in palladium dispersion or distribution. Therefore, observable changes of the Pd $3d_{5/2}$ binding energy and the Auger parameter may be ascribed primarily to the replacement of protons by Na^+ or NH_4^+ ions, and thus to the disappearance of electron sharing between metal atoms and protons. Taking into account that the total shift in binding energy of the Pd $3d_{5/2}$ line in reduced Pd/NaY before neutralization relative to that of the bulk metal is 1.0 eV, and after neutralization 0.6 eV, we can estimate the shift due to electron transfer as ca. 0.4 eV. The effect due to the small particle size amounts to ca. 0.6 eV. This value agrees well with results obtained for Pd on inert supports. Ryndin et al.[39] showed that for Pd/SiO_2 and Pd/Al_2O_3 an increase in the size of the Pd particles from 1.0 to 4.0 nm led to a shift of the Pd $3d_{5/2}$ level by 0.6 eV. Our conclusion that the shift due to the positive charge of Pd in $[Pd_n-H_m]^{m+}$ adducts amounts to 0.3–0.4 eV thus appears consistent with their estimation of the shift due to the size effect.

The modified Auger parameter differs significantly for samples neutralized with either NH_3 or NaOH. We propose the following explanation for this phenomenon. Changes in the modified Auger parameter reflect mainly the change in the electronic response of the environment of the atom to the creation of the core hole.[40,41] Kohiki showed that for Pd clusters evaporated on different supports α' is sensitive to the polarizability of the support.[23] It is tempting to relate the observable shift in α' with the substitution of protons in close proximity to the Pd clusters by more polarizable Na^+ and by even more polarizable NH_4^+. The observable α' value increases with the increasing polarizability of the neighbouring ions ($0 \approx H^+ \ll Na^+ < NH_4^+$) and reflects modification of the Pd cluster environment.

Varying the charge-compensating ion also results in a shift of the Pd $3d_{5/2}$ binding energy of Pd/NaY, Pd/HY and Pd/MgY (Table 2, Fig. 5 and 6). For Pd/HY and Pd/MgY the shifts are 0.4 eV higher than that for Pd/NaY. As determined by TPD, the dispersions of Pd on these samples are similar; we can thus conclude that the additional shift arises mainly from electron donation from the metal to protons. Correspondingly, the positive charge of the metal clusters on HY and MgY is twofold higher than on NaY.

These conclusions are further substantiated by previous TPR results.[29] In Pd/MgY Mg^{2+} ions occupy mainly small cages because this location is thermodynamically preferred owing to the high density of negative charge in the small zeolite cages. Consequently the Pd^{2+} ions will remain in the supercages during calcination; the protons which are formed during reduction remain in the supercages which they share with Pd particles. The situation in Pd/NaY is different: during calcination at 500 °C the Pd^{2+} ions migrate into the sodalite cages in exchange for Na^+ ions. During reduction at high T_R the Pd atoms migrate into the supercages leaving the protons behind. Although these protons are also able to migrate themselves to the supercages, the absence of divalent cations will result in a distribution of the protons over the available positions, with a much lower occupancy of supercage sites than in the case of MgY. The present finding that Pd clusters are much more electron-deficient in Pd/MgY than in Pd/NaY thus fully confirms the model which actually motivated these experiments.

The fact that increasing proton concentration around a Pd cluster increases the electron deficiency of the cluster suggests that several acceptor sites share electrons with the metal particle, viz. a given Pd_n cluster might interact with more than one proton. If the increase of the observed positive charge on the Pd cluster arose only from a shift of the equilibrium $Pd_n + H^+ \rightleftharpoons [Pd_n-H]^+$ towards the proton adduct with increasing H^+ concentration, one would expect broadening of the Pd 3d line (or even splitting) owing to the presence of two types of Pd species. However, the FWHH of the Pd $3d_{5/2}$ line remains constant (Tables 1 and 2); only the binding energy increases with increasing number of protons surrounding the Pd particle. This suggests that an increase in the positive charge of the $[Pd_n-H_m]^{m+}$ adduct results from an increase in the value of m; the charge associated with all proton adducts at a given H^+ concentration remains relatively uniform.

It is remarkable that the Auger parameter for Pd/HY and Pd/MgY not only differs from that for Pd/NaY, but also differs between Pd/HY and Pd/MgY. These differences indicate changes in the environment of the metal particles. The α' values show the same trend as the polarizabilities of the charge-compensating ions: 661.7 eV for protons in HY, 662.0 eV for a combination of protons and Mg^{2+} ions in supercages of reduced Pd/MgY, 662.3 eV for a combination of Na^+ ions with the same protons in reduced Pd/NaY, 662.6 eV for the Na^+ ions in reduced and neutralized Pd/NaY and 663.0 eV for combination of Na^+ and NH_4^+ ions in Pd/NaY neutralized with ammonia. Presumably, the Auger parameter shift depends not only on proton concentration in the vicinity of the Pd clusters (as for the Pd $3d_{5/2}$ binding energy), but also on the polarizability of the other cations. Thus, additional information on the Pd cluster environment can be obtained from the Auger parameter shifts.

Conclusion

The extent of the electron deficiency of Pd clusters in Y zeolite with varying proton concentrations and locations has been identified by XPS. The contribution of an intrinsic size effect has been separated from that due to a real transfer of

electron density from metal particles to zeolite protons. The electron sharing between Pd clusters and protons in Pd/NaY results in an upward shift of the binding energy of Pd $3d_{5/2}$ of ca. 0.4 eV. The positive charge of the Pd clusters in HY and MgY exceeds that in Pd/NaY by a factor of two. For HY this is due to the high overall proton concentration, but in MgY the 'site-blocking' effect of the Mg^{2+} ions directs protons specifically to the supercages where the Pd clusters are located. The Auger parameter reflects mainly the structure of the immediate environment of the metal clusters. An increase in the number of protons interacting with the metal particle results in a decrease of α'. Upon replacing protons by polarizable ions (Mg^{2+}, Na^+, NH_4^+) the parameter α' gradually increases with their polarizability. All data agree with the basic model that the electron deficiency of Pd in zeolites is due to the formation of proton adducts $[Pd_n-H_m]^{m+}$ with $m \geq 1$.

References

1 J. A. Rabo, P. E. Pickert, D. N. Stauires and J. E. Bogle, *Actes Deuxieme Congr. Int. Catal.*, Paris, 1961, Ed. Technip, Paris, 1961, vol. 2, p. 2055.
2 Kh. M. Minachev and Ya. I. Isakov, in *Zeolite Chemistry and Catalysis*, ed. J. A. Rabo, ACS, Washington DC, 1976, p. 552.
3 Ya. I. Isakov and Kh. M. Minachev, *Russ. Chem. Rev.*, 1982, **51**, 1182.
4 J. Scott, *Zeolite Technology and Application*, Noyes Data Corp., 1980.
5 I. E. Maxwell, *Adv. Catal.*, 1982, **31**, 2.
6 P. Gallezot, J. Datka, J. Massardier, M. Primet and B. Imelik, in *Proc. 6th Int. Congr. Catal.*, ed. G. C. Bond *et al.*, The Chemical Society, London, 1977, p. 696.
7 J. Bandiera, *J. Chim. Phys.*, 1980, **77**, 303.
8 V. N. Romannikov, K. G. Ione and L. A. Pedersen, *J. Catal.*, 1980, **66**, 121.
9 R. A. Dalla Betta and M. Boudart, in *Proc. 5th Int. Congr. Catal.*, ed. H. Hightower, North Holland, Amsterdam, 1973, p. 1329.
10 C. Naccache, N. Kaufherr, M. Dufaux, J. Bandiera and B. Imelic, in *Molecular Sieves-II*, ed. J. R. Katzer, ACS, Washington DC, 1977, p. 538.
11 S. T. Homeyer, Z. Karpiński and W. M. H. Sachtler, *J. Catal.*, 1990, **123**, 60.
12 S. T. Homeyer, Z. Karpiński and W. M. H. Sachtler, *Recl. Trav. Chim. Pays-Bas*, 1990, **109**, 81.
13 X. Bai and W. M. H. Sachtler, *J. Catal.*, 1900, **129**, 121.

14 T. M. Tri, J. Massardier, P. Gallezot and B. Imelik, in *Catalysis by Zeolites*, ed. B. Imelik *et al.*, Elsevier, Amsterdam, 1980, p. 279.
15 T. M. Tri, J. P. Candy, P. Gallezot, J. Massardier, M. Primet, J. C. Vedrine and B. Imelik, *J. Catal.*, 1983, **79**, 396.
16 W. M. H. Sachtler, in *Chemistry and Physics of Solid Surfaces*, ed. R. Vanselov and R. Howe, *Springer Ser. Surf. Sci. 22*, Springer-Verlag, Berlin, 1990, p. 69.
17 Z. Karpiński, S. T. Homeyer and W. M. H. Sachtler, in *Structure–Activity and Selectivity Relationships in Heterogeneous Catalysis*, ed. R. K. Grasselli and A. Sleight, Elsevier, Amsterdam, 1991, p. 203.
18 T. T. Phuong, J. Massardier and P. Gallezot, *J. Catal.*, 1986, **102**, 456.
19 J. C. Védrine, M. Dufaux, C. Naccache and B. Imelik, *J. Chem. Soc., Faraday Trans. 1*, 1978, **74**, 440.
20 M. Narayana, J. Michalik, S. Contarini and L. Kevan, *J. Phys. Chem.*, 1985, **89**, 3895.
21 G. V. Antoshin, E. S. Shpiro, O. P. Tkachenko, S. B. Nikishenko, M. A. Ryashentseva, V. I. Avaev and Kh. M. Minachev, in *Proc. 7th Int. Congr. Catal.*, ed. T. Seiyama and K. Tanabe, Elsevier, Amsterdam, 1981, p. 302.
22 M. G. Mason, *Phys. Rev. B*, 1983, **27**, 748.
23 S. Kohiki, *Appl. Surf. Sci.*, 1986, **25**, 81.
24 G. K. Wertheim, *Z. Phys. D*, 1989, **12**, 319.
25 L. L. Sheu, H. Knözinger and W. M. H. Sachtler, *J. Am. Chem. Soc.*, 1989, **111**, 8125.
26 C. D. Wagner, *Faraday Discuss. Chem. Soc.*, 1975, **60**, 291.
27 C. D. Wagner and A. Joshi, *J. Electron Spectrosc. Relat. Phenom.*, 1988, **47**, 283.
28 S. T. Homeyer and W. M. H. Sachtler, *J. Catal.*, 1989, **117**, 91.
29 S. T. Homeyer and W. M. H. Sachtler, *J. Catal.*, 1989, **118**, 266.
30 Z. Zhang, T. Wong and W. M. H. Sachtler, *J. Catal.*, 1991, **128**, 13.
31 C. D. Wagner, L. E. Davis, M. V. Zeller, J. A. Taylor, R. H. Raymond and L. H. Gale, *Surf. Interface Anal.*, 1981, **3**, 211.
32 Kh. M. Minachev, G. V. Antoshin and E. S. Shpiro, *Izv. Akad. Nauk SSSR, Ser. Khim.*, 1974, 101.
33 T. Reich, V. G. Yarzemski and V. I. Nefedov, *J. Electron Spectrosc. Relat. Phenom.*, 1988, **46**, 255.
34 D. W. Breck, *Zeolite Molecular Sieves*, Robert E. Krieger Publishing Company, Malaber, Florida, 1984, p. 145.
35 G. Bergeret, P. Gallezot and B. Imelik, *J. Phys. Chem.*, 1981, **85**, 411.
36 Z. Zhang, H. Chen, L. Sheu and W. M. H. Sachtler, *J. Catal.*, 1991, in the press.
37 T. D. Thomas, *J. Electron Spectrosc. Relat. Phenom.*, 1980, **20**, 117.
38 G. K. Wertheim, *Phys. Rev. B*, 1987, **36**, 9559.
39 Yu. A. Ryndin, L. V. Nosova, A. I. Boronin and A. L. Chuvilin, *Appl. Catal.*, 1988, **42**, 131.
40 R. H. West and J. E. Castle, *Surf. Interface Anal.*, 1982, **4**, 68.
41 G. Moretti, *Surf. Interface Anal.*, 1990, **16**, 159.